Adulis and the transshipment of baboons during classical antiquity

Franziska Grathwol[1], Christian Roos[2], Dietmar Zinner[3,4,5], Benjamin Hume[1,6], Stéphanie M. Porcier[7], Didier Berthet[8], Jacques Cuisin[9], Stefan Merker[10], Claudio Ottoni[11], Wim Van Neer[12,13], Nathaniel J. Dominy[14,15], Gisela H. Kopp[1,15,16,17,*]

[1] Department of Biology, University of Konstanz, Konstanz, Germany
[2] Gene Bank of Primates and Primate Genetics Laboratory, Deutsches Primatenzentrum, Leibniz Institute for Primate Research, Göttingen, Germany
[3] Cognitive Ethology Laboratory, Deutsches Primatenzentrum, Leibniz Institute for Primate Research, Göttingen, Germany
[4] Department of Primate Cognition, Georg-August-University of Göttingen, Göttingen, Germany
[5] Leibniz-ScienceCampus Primate Cognition, Göttingen, Germany
[6] SequAna – Sequencing Analysis Core Facility, University of Konstanz, Konstanz, Germany
[7] Laboratoire CNRS ASM ≪ Archéologie des Sociétés Méditerranéennes (UMR 5140), Université Paul-Valéry, LabEx Archimede, Montpellier, France.
[8] Musée des Confluences, Lyon, France
[9] Muséum National d'Histoire Naturelle, Paris, France
[10] Department of Zoology, State Museum of Natural History Stuttgart, Germany
[11] Department of Biology, University of Rome Tor Vergata, Rome, Italy
[12] Royal Belgian Institute of Natural Sciences, Brussels, Belgium
[13] Department of Biology, KU Leuven, Leuven, Belgium
[14] Departments of Anthropology and Biological Sciences, Dartmouth College, Hanover, USA
[15] Zukunftskolleg, University of Konstanz, Konstanz, Germany
[16] Department of Migration, Max Planck Institute of Animal Behavior, Konstanz, Germany
[17] Centre for the Advanced Study of Collective Behaviour, University of Konstanz, Konstanz, Germany

* Corresponding author: gisela.kopp@uni-konstanz.de

Abstract

30 Adulis, located on the Red Sea coast in present-day Eritrea, was a bustling trading centre

31 between the first and seventh centuries CE. Several classical geographers—Agatharchides

32 of Cnidus, Pliny the Elder, Strabo—noted the value of Adulis to Greco-Roman Egypt,

33 particularly as an emporium for living animals, including baboons (*Papio* spp.). Though

34 fragmentary, these accounts predict the Adulite origins of mummified baboons in Ptolemaic

35 catacombs, while inviting questions on the geoprovenance of older (Late Period) baboons

36 recovered from Gabbanat el-Qurud ("Valley of the Monkeys"), Egypt. Dated to ca. 800–540

37 BCE, these animals could extend the antiquity of Egyptian-Adulite trade by as much as five

38 centuries. To explore this possibility, we analysed complete mitochondrial genomes from a

39 mummified baboon from Gabbanat el-Qurud and 14 museum specimens with known

40 provenance together with published georeferenced mitochondrial sequence data.

41 Phylogenetic assignment connects the mummified baboon to modern populations of *Papio*

42 *hamadryas* in Eritrea and eastern Sudan. This result, assuming geographical stability of

43 phylogenetic clades, suggests that present-day Eritrea, and by extension Adulis, was a source

44 of baboons for Late Period Egyptians. It also establishes geographic continuity with baboons

45 from the fabled Land of Punt (Dominy et al., 2020), giving weight to speculation that Punt and

46 Adulis were essentially the same trading centres separated by a thousand years of history.

47

Key words

49 *Papio*; ancient DNA; ancient trade routes; phylogeography; mitochondrial genome;

50 museomics; capture enrichment

51

Introduction

Adulis, on the coast of present-day Eritrea, was an important hub during the rise of cross-ocean maritime trade, connecting ships, cargoes, and ideas from Egypt, Arabia, and India (Burstein, 2002; Munro-Hay, 1982; Seland, 2008). Trade peaked between the fourth and seventh centuries CE, propelling the rise and expansion of the Aksumite kingdom, but its occupation history extends, at minimum, to the first millennium BCE (Zazzaro et al., 2014). Corroborating this archaeological record are written accounts that draw attention to the importance of Adulis as one of the foremost sources of African animals or animal products during the Hellenistic period (323–31 BCE). In *Topographia Christiana*, a sixth-century text, the Nestorian merchant Cosmas Indicopleustes recounts his own visit to Adulis in 518 CE (Fauvelle-Aymar, 2010; Hatke, 2013). There he copied the text of a stele inscribed in Ge'ez and Greek, and known today as the *Monumentum Adulitanum I*. The text celebrates the military conquests of Ptolemy III Euergetes [reign: 246–222 BCE] and notes the local availability of war elephants for himself and his predecessor, Ptolemy II Philadelphus [reign: 284–246 BCE] (Bowersock, 2013).

Echoing this account is the first-century *Periplus Maris Erythraei*, an anonymous text focused on maritime trade across the Red Sea Basin: "practically the whole number of elephants and rhinoceros that are killed live in the places inland, although at rare intervals they are hunted on the seacoast even near Adulis" (Casson, 1989, 1993). Pliny the Elder described Adulis as a thriving emporium in his *Naturalis Historia*, another first-century text, and commented on the availability of ivory, rhinoceros horn, hippopotamus hides, tortoise shell, and *sphingia*—or 'sphinx monkeys,' a term that probably refers to the gelada, *Theropithecus gelada* (Jolly & Ucko, 1969). Pliny's account relied heavily on the writings of Agatharchides of Cnidus (ca.145 BCE), who described 'Aithiopia' (meaning the Red Sea coast and African hinterlands) as a source of sphinx monkeys, *cepi* (probably patas monkeys, *Erythrocebus patas* (Burstein, 1989)), and *cynocephali*–or 'dog-heads'. Strabo's *Geographica* references the worship of *cynocephali* at Hermopolis (Egypt), making it clear that the animal in question is the hamadryas baboon (*Papio hamadryas*)*,* the traditional sacred animal of the Egyptian god Thoth (Figure 1). The source of baboons in ancient Egypt is an enduring question (Dominy et al., 2020), as the current distribution of baboons excludes Egypt (Figure 2) and there is no prehistoric evidence of baboons occurring in Egypt naturally (Geraads, 1987).

Figure 1. Strabo's reference (17.1.40) to the worship of cynocephali at Hermopolis Magna makes clear that the animal in question is the hamadryas baboon (*Papio hamadryas*). The sanctuary and temple complex featured several 35-ton statues of *P. hamadryas* as the embodiment of Thoth. One of the oldest deities in the Egyptian pantheon, Thoth is best known as a god of writing and wisdom, a lunar deity, and vizier of the gods, but also as a cosmic deity, creator god, and warrior (Stadler, 2012). The quartzite statues were erected by Amenhotep III, 18th Dynasty, New Kingdom, 1390-1353 BCE. Photograph by N.J. Dominy.

Though fragmentary, the outlined historiography points to Adulis as a commercial source of mummified baboons in Ptolemaic catacombs, such as those at Saqqara and Tuna el-Gebel (Goudsmit & Brandon-Jones, 1999; Peters, 2020) [or those of their progenitors if Ptolemaic Egyptians maintained captive breeding programs (von den Driesch et al., 2004)]. At the same time, these accounts invite questions focused on the source of pre-Ptolemaic baboons recovered from Gabbanat el-Qurud, Egypt (Lortet & Gaillard, 1907) and dated to ca. 800–540 BCE (Richardin et al., 2017), a span that corresponds to the 25th Dynasty and Late Period of Egyptian antiquity. If these specimens can be traced to Eritrea, and by extension Adulis, then

100 they have the potential to extend the time depth of Egyptian-Adulite trade by as much as five
101 centuries.

102 Mummified baboons have been investigated morphologically, revealing species-level
103 taxonomic assignments as well as individual details, such as age, sex, and pathological
104 condition (Boessneck, 1987; Brandon-Jones & Goudsmit, 2022; Goudsmit & Brandon-Jones,
105 1999, 2000; Peters, 2020). Such data are telling, but insufficient for determining fine-scale
106 geographic origins. Recent oxygen and strontium stable isotope evidence suggest that
107 mummified hamadryas baboons were imported from the region of northern Somalia, Eritrea
108 and Ethiopia (Dominy et al., 2020). However, this method is not capable of pinpointing the
109 geographic location of origin more precisely. It also fails at determining the geoprovenance of
110 earlier generations bred in captivity, as shown for olive baboons from the Ptolemaic catacombs
111 of North Saqqara (Dominy et al., 2020). The analysis of ancient DNA (aDNA) recovered from
112 baboon mummies and compared to the current distribution of baboon genetic diversity has
113 the potential to provide more detailed insights on the geographic origin of baboons in ancient
114 Egypt. To explore this possibility, we sequenced the mitochondrial genome (mitogenome) of
115 a mummified baboon to infer its geographic origin through phylogenetic assignment.

116

117 **Materials and Methods**

118 In *Topography of Thebes*, Wilkinson (1853) noted a site called Gabbanat el-Qurud ("Valley of
119 the Monkeys") located ca. 2.5 km north-northwest of Medinet Habu, the mortuary temple of
120 Ramses III. Intrigued by this observation, French Egyptologists Louis Lortet and Claude
121 Gaillard sought and found the site in February 1905, along with the remains of mummified
122 baboons. They recovered "seventeen skulls and a large quantity of bones," which they
123 attributed to *P. anubis* and *P. hamadryas* (Lortet & Gaillard, 1907, 1909). The assemblage
124 includes juvenile and adult males and females buried in jars, sarcophagi, or wooden coffins.
125 Now accessioned in the Musée des Confluences, Lyon, France, the linen wrapping of one
126 mummified individual (MHNL 90001206) is dated radiometrically to 803 (95.4%) 544 cal. BC
127 (Richardin et al., 2017).

128 Ottoni et al. (2019) sampled dental calculus from 16 individuals in this assemblage and
129 reported the preservation of ancient microbial DNA in a subset of six. Their success motivated
130 us to extract DNA from the remaining tooth material of ten individuals (Table 1, Table S1). In
131 addition, we obtained samples (skin, bone or tooth) from 21 modern historic specimens of
132 baboons available in museum collections and representing the northeast African distribution

5

133   of the genus *Papio* (Table 1, Figure 2). These specimens were collected between 1855 and

134   1978 and we denote them "historic samples" in the remainder of the manuscript to distinguish

135   them both from the older mummified specimens ("mummified samples") and recently collected

136   material ("modern samples"). Latitude-longitude information on the origin of the specimens

137   was either derived from the respective museum database or assigned based on the listed

138   provenance (Table 1).

139

140
141
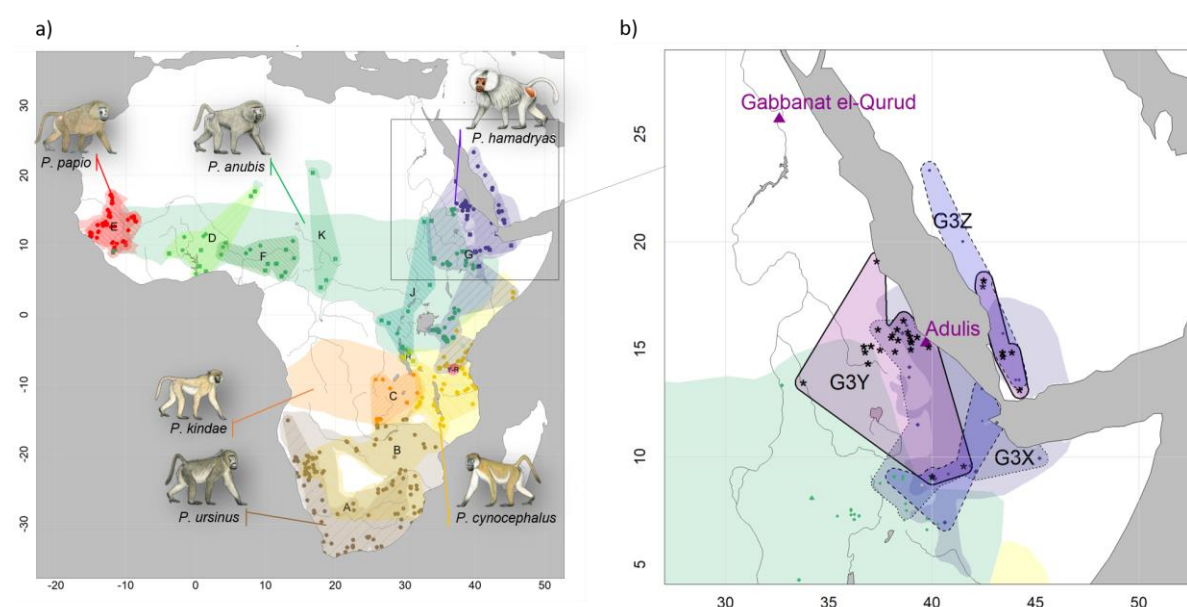
142   **Figure 2: Present-day distributions of the six baboon species, major mitochondrial clades, and provenance**

143   **of samples analysed in this study.** a) Overview of species distributions according to the IUCN (2020) and

144   coloured by species (red: *P. papio*, brown: *P. ursinus*, yellow: *P. cynocephalus*, orange: *P. kindae*, green: *P. anubis*,

145   purple: *P. hamadryas*). Colour-patterned regions reflect main mitochondrial clade attribution resulting from

146   phylogenetic reconstructions and are denoted with capital letters A-K (cf. Figure 3). Squares and circles represent

147   geoprovenance of mitogenomes and partial mtDNA datasets (e.g. D-loop, cytochrome *b*), respectively, and are

148   coloured by species. Note that introgressive hybridization has led to discordances between species assignment

149   and mitochondrial clades. b) Close-up of the distribution of mitochondrial subclades G3-X, G3-Y, and G3-Z in the

150   north-eastern distribution of baboons. Samples attributed to G3-Y, the subclade assigned to the mummified baboon

151   in phylogenetic reconstructions and haplotype networks, are highlighted with asterisks. The locations of the

152   excavation site of the mummified baboon, Gabbanat el-Qurud, and Adulis are marked with magenta triangles. Male

153   baboon drawings by Stephen Nash, used with permission.

154

155   *DNA extraction and sequencing*

156   DNA damage and degradation is expected from ancient (mummified) and 19th/early 20th

157   century museum specimens. We therefore analysed mitochondrial DNA (mtDNA), which is

158   available in higher copy numbers than nuclear DNA and holds greater potential for success

6

when sample quality is poor. We analysed complete mitogenomes because they are effective for reconstructing robust mitochondrial phylogenies of modern baboons and have proven to indicate the geographic origin of the corresponding sample reliably (Roos et al., 2021; Zinner et al., 2013). Recent advances in sequencing technologies allow the successful sequencing of mitogenomes either with a shotgun sequencing approach or, for samples with very low DNA quality and quantity, with a capture enrichment approach (Schuenemann et al., 2017; Shapiro & Hofreiter, 2013).

We extracted DNA with a specific column-based method aimed at the recovery of short DNA fragments following established protocols and necessary precautions for the analysis of aDNA (Dabney, Knapp, et al., 2013; Rohland et al., 2004; Roos et al., 2021). In particular, samples from mummified specimens were extracted separately and in a dedicated aDNA laboratory to prevent cross-contamination. Concentration of DNA extracts was measured on a Qubit fluorometer (Life Technologies, Singapore) and quality checked on a Bioanalyzer (Agilent, Santa Clara, US) or Tapestation 2200 (Agilent). All samples were initially sequenced with a shotgun approach. Samples with DNA extract concentrations below 4.5ng/µl or final mitogenome sequencing depth below 10X, and with enough remaining DNA extract, were enriched for mtDNA with a capture approach.

For the shotgun approach, sequencing libraries were prepared with the NEBNext Ultra II DNA Library Prep Kit (New England BioLabs, Frankfurt, Germany) according to the manufacturer's instructions without prior fragmentation. Library concentration and quality were assessed with the Qubit Fluorometer and Bioanalyzer and molarity was estimated via qPCR with the NEBNext Library Quant Kit (New England Biolabs). Libraries were single indexed with NEBNext Multiplex Oligos (New England Biolabs) with 5-11 PCR cycles and cleaned up with the kit's beads.

For the capture enrichment approach, RNA baits (myBaits custom Kit, Arbor Biosciences, Ann Arbor, USA) were designed for the mitogenome of *P. anubis* East (GenBank Acc. No. JX946196; (Zinner et al., 2013)). We prepared libraries with the Accel-NGS 1S Plus DNA Library Kit and the 1S Plus Dual Indexing Kit (Swift Biosciences, Ann Arbor, USA) according to the manufacturer's instructions for small fragment retention. Hybridization capture was performed with a 48h incubation step according to the manufacturer's instructions for highly degraded DNA. After library amplification with 14 PCR cycles, libraries were cleaned with SPRIselect beads (Beckmann Coulter, Krefeld, Germany).

Sequencing was performed with 24 libraries per lane (23 samples + pooled negative control to monitor contamination) on an Illumina HiSeq4000 (50bp, single-end read) at the NGS

7

193   Integrative Genomics core unit of the University Medical Center Göttingen, Göttingen,

194   Germany, or on a NovaSeq6000 SP flow cell (100bp, paired-end read) at the Max Planck

195   Institute for Molecular Genetics, Berlin, Germany. Capture enrichment libraries were reloaded

196   and sequenced a second time to increase the number of reads.

197

198   *Mitogenome assembly*

199   Raw sequencing reads were demultiplexed and adapters trimmed at the sequencing facilities.

200   We performed subsequent sequence processing on the central high performance computing

201   cluster bwForCluster BinAC. We checked read quality with FastQC 0.11.8 (Andrews, 2010),

202   trimmed and filtered reads with Trimmomatic 0.39 (Bolger et al., 2014) using the settings

203   ILLUMINACLIP:TruSeq3-PE.fa:2:30:10 MINLEN:30 SLIDINGWINDOW:4:20 LEADING:20

204   TRAILING:20, AVGQUAL:30, and confirmed adequate quality of trimmed reads again with

205   FastQC. Reads were mapped with Burrows Wheeler Aligner (BWA) backtrack 0.7.17 (Li &

206   Durbin, 2009) using default settings independently to each of seven different mitogenomes of

207   representatives of the northern baboon clades (*P. anubis* East JX946196; *P. anubis* Gombe

208   MG787545; *P. anubis* West1 JX946197; *P. anubis* West 2 JX946198; *P. cynocephalus* North

209   JX946199; *P. hamadryas* JX946201; *P. papio* JX946203). We chose this approach to avoid

210   biases in downstream analyses introduced through the choice of the reference genome and

211   used the consensus sequence resulting from the best mapping results in downstream

212   analyses. We did not adjust the settings as usually recommended to improve mapping results

213   for aDNA (Schubert et al., 2012) but were stringent in mapping and filtering of reads to avoid

214   the inclusion of nuclear mitochondrial DNA segments (NUMTs). Alignments were indexed with

215   SAMtools 1.10 "index" and filtered with "view" for mapped and (in the case of paired-end data)

216   properly paired reads with a mapping quality of at least MAPQ 30. Library complexity was

217   estimated with the "EstimateLibraryComplexity" from the Picard Toolkit 2.20.4 (Broad Institute,

218   2019). We merged BAM files of the same samples with "MergeSamFiles" and removed

219   duplicates with "MarkDuplicates" from the Picard Toolkit. DNA damage was estimated

220   calculating the frequency of base substitutions, insertions and deletions at the 5' and 3' end,

221   respectively, with DamageProfiler 1.0 (Neukamm et al., 2021). We calculated average

222   sequencing depth with SAMtools 1.10 "depth" (Li et al., 2009) as the sum of reads covering

223   each position divided by the number of bases in the reference genome, and estimated GC-

224   bias with "CollectGCBiasMetrics" from the Picard Toolkit. We created a consensus sequence

225   for each sample with the "doFasta" option in ANGSD (Korneliussen et al., 2014) using the

226   base with the highest effective depth (EBD) and setting positions with coverage below 2 to

227 undetermined. We only retained mitogenomes for further analyses for which at least 80% of
228 the sequence were covered at 3X.

229 We augmented our dataset with published mitogenomes of baboons (Roos et al., 2021) and
230 *T. gelada* as outgroup (Table 1), and aligned sequences with MUSCLE 3.8.81 (Edgar, 2004)
231 as implemented in the package msa 1.28.0 (Bodenhofer et al., 2015) in R 4.2.1 (R Core Team,
232 2022) using standard settings with a maximum number of 16 iterations.

233 For a more fine-scale geographic representation, we further included published sequence data
234 from the north-eastern part of the baboon distribution of two different mitochondrial markers
235 with differing resolution: the cytochrome *b* gene (cyt *b*) (Zinner et al., 2009, 2015), and a
236 fragment of the hypervariable region I (HVRI) of the D-loop (Hapke et al., 2001; Kopp, Ferreira
237 da Silva, et al., 2014; Kopp, Roos, et al., 2014; Städele et al., 2015; Winney et al., 2004). We
238 extracted the corresponding regions from the mitogenome alignment and again removed
239 sequences with more than 10% undetermined sites.

240

241 *Phylogenetic reconstruction*

242 To identify the phylogenetic affiliation of the newly investigated samples, we reconstructed
243 phylogenetic trees based on the final dataset of 46 mitogenomes (alignment length: 16,628bp)
244 using Maximum Likelihood (ML) and Bayesian inference (BI) methods with W-IQ-Tree 1.6.12
245 (Nguyen et al., 2015; Trifinopoulos et al., 2016) and MrBayes 3.2.7 (Huelsenbeck & Ronquist,
246 2001; Ronquist & Huelsenbeck, 2003), respectively. We treated the mitogenome as a single
247 partition, the optimal substitution model for phylogenetic reconstructions was detected to be
248 TN+F+I+G4 (Tamura & Nei, 1993) under the Bayesian information criterion (BIC) and
249 GTR+F+I+G4 (Tavaré, 1986) under the Corrected Akaike Information Criterion (AICc) with
250 Modelfinder (Kalyaanamoorthy et al., 2017) as implemented in W-IQ-Tree. The ML tree was
251 reconstructed with 10,000 ultrafast bootstrap replications (Hoang et al., 2018) applying the
252 TN+F+I+G4 model. The BI tree was reconstructed applying the GTR+I+G model and using
253 four independent Markov chain Monte Carlo (MCMC) runs with 1 million generations, a burn-
254 in of 25% and sampling every 100 generations. To ensure convergence, the Potential Scale
255 Reduction Factor (PSRF) was checked to be close to 1 for all parameters. We visualized
256 phylogenetic trees with the R package ggtree 3.4.2 (Yu et al., 2017) and adopted clade
257 nomination of (Roos et al., 2021) and (Kopp, Roos, et al., 2014).

258

259 *Haplotype networks*

260 To determine the mitochondrial clade of origin of the analysed samples more precisely, we

261 reconstructed median-joining haplotype networks (Bandelt et al., 1999) with Popart 1.7 (Leigh

262 & Bryant, 2015) for both the HVRI (n=644, 176bp) and the cyt *b* (n=137, 1140bp) dataset.

263

264 *Geographic maps*

265 Geographic maps were created in R. We obtained species distribution shapefiles from IUCN

266 (Gippoliti, 2019; Sithaldeen, 2019; Wallis, 2020a, 2020b; Wallis et al., 2020; Wallis et al.,

267 2021), river, lake and coastlines from Natural Earth (https://www.naturalearthdata.com) via

268 rnaturalearth 0.1.0 (Massicotte & South, 2023).

269

270 **Results**

271 *Mitogenomes from mummified and historic specimens*

272 We discarded seven historic samples and nine mummified samples from our analysis due to

273 insufficient DNA content, sequencing failure or low coverage and sequencing depth (Table

274 S1). Thus, our results are based on the newly generated mitogenomes of 14 historic and one

275 mummified individual (Table 1). In total, we obtained 896,025,770 raw sequence reads, with

276 a mean of 34,462,530 (±SD 27,945,321) raw sequence reads per sample. On average 95.5%

277 of reads survived trimming and a median of 9,934 (range: 244 – 2,722,354) reads per sample

278 mapped to the reference genome. After removal of duplicates (duplication level median:

279 25.1%, range: 2.5 – 92.6%), a median of 7,398 (range: 237 – 497,458) mapped reads per

280 sample resulted in the median final sequencing depth of 26X (range: 0.21 – 2952X). After

281 exclusion of samples with low quality, the final dataset had a median final sequencing depth

282 of 37X (range: 16 – 2952X), with a median of 0.4% undetermined sites (range: 0 – 1.7%) and

283 a median breadth of coverage of at least 3X of 99.3% (range: 97.4 – 100%) (Table S1). All

284 these metrics differed considerably depending on sample age (historic versus mummified) and

285 DNA concentration (Figures S1 & S2). Capture enrichment strongly increased the number of

286 mapped reads and final mean coverage as compared to the shotgun approach (Figures S1 &

287 S2). GC-content of sequences was 40 - 50% (Figure S3), in the same range as the reference

288 genomes.

289   The sequencing reads of the mummified sample (MHNL51000172) exhibit C to T and G to A

290   misincorporations at 5' and 3' ends, reaching frequencies of 3.3% and 1.6% at the first/last

291   position of the read (Figure S4).

292

293   *Phylogenetic mapping*

294   Phylogenetic trees inferred from ML and BI revealed identical topologies with generally strong

295   node support (100% Bootstrap support (BS) and posterior probability (PP) 1.0) and clearly

296   defined geographic clades (Figures 3 & S5). These mitochondrial clades did not directly mirror

297   species assignments. Within the north-eastern baboons, the central olive baboon clade J from

298   Democratic Republic of the Congo, Tanzania, South Sudan and southern Sudan diverged first,

299   followed by northern yellow baboons of clade G1 including a sample from Somalia.

300   Hamadryas baboons formed clade G3, which also included olive baboons from the region.

301   Clade G3 contained three subclades: Subclade G3-Z comprised hamadryas baboons from

302   Ethiopia and Djibouti, subclade G3-X comprised hamadryas and olive baboons from Ethiopia,

303   Eritrea, and Somalia, and subclade G3-Y comprised hamadryas and olive baboons from north-

304   eastern Sudan and Eritrea. The mummified baboon from Gabbanat el-Qurud (MHNL

305   51000172) was located in subclade G3-Y, closest related to samples from Eritrea and north-

306   eastern Sudan.

307

11
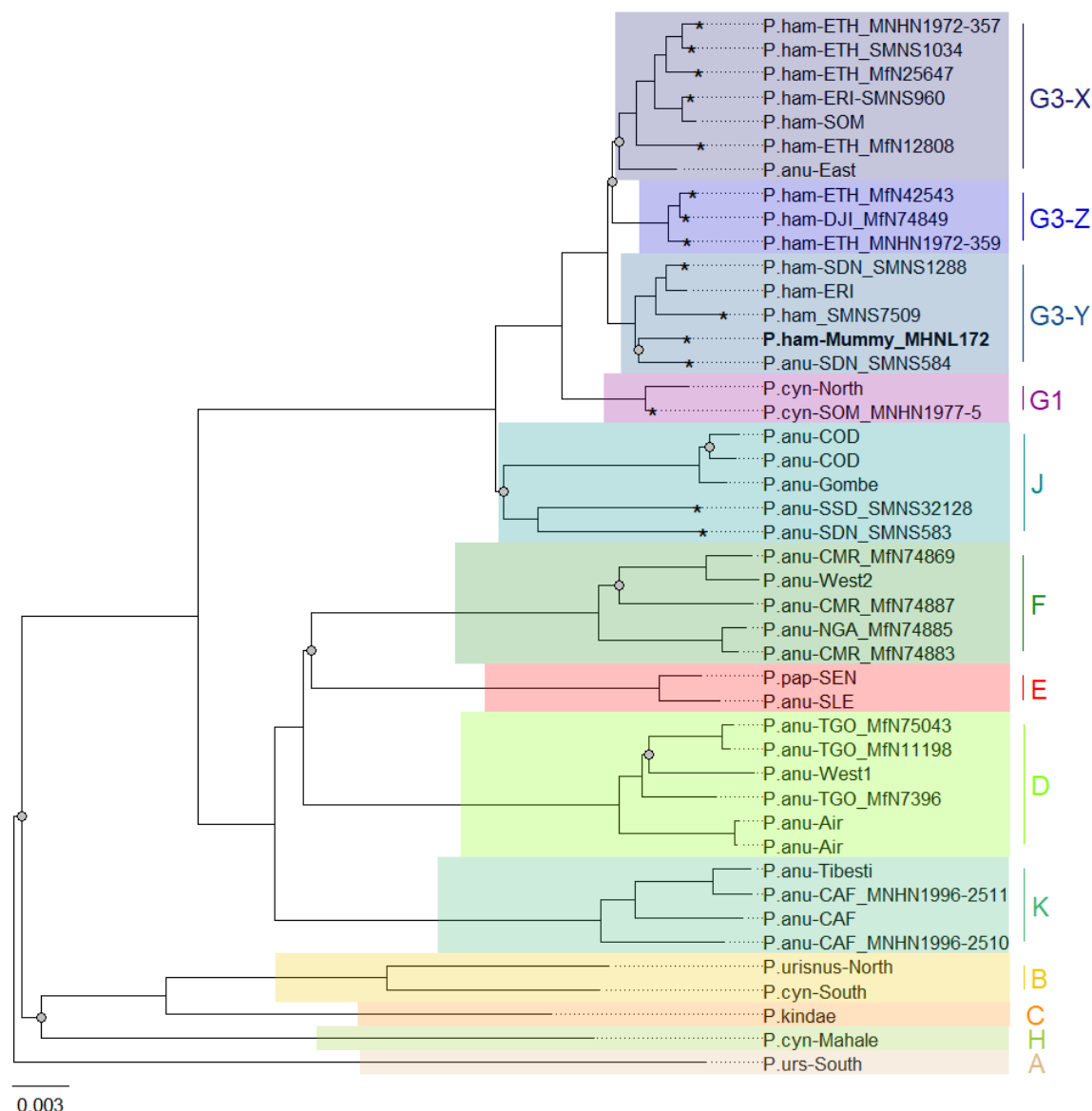
Figure 3: Phylogeny of baboons based on complete mitochondrial genomes as inferred from Maximum Likelihood analysis. *P. cynocephalus* from the Udzungwa Mountains and outgroup *T. gelada* were omitted from visualization for clarity. The analysed baboon mummy sample MHNL 51000172 (in bold) falls into clade G3-Y. Clade names (A-K) according to Roos et al. (2021), subclades X - Z according to Kopp et al. (2014); sample IDs include putative species (P.ham - *P. hamadryas*, P.anu - *P. anubis*, P.cyn - *P. cynocephalus*, P.urs - *P. ursinus*, P.pap - *P. papio*), country of origin code (CAF - Central African Republic, CMR - Cameroon, COD - Democratic Republic of Congo, DJI - Djibouti, ERI - Eritrea, ETH - Ethiopia, NGA - Nigeria, SDN - Sudan, SSD - South Sudan, SEN - Senegal, SLE - Sierra Leone, SOM - Somalia, TGO - Togo; note that sample SMNS7509 is of unclear geoprovenance) and abbreviated museum code. Nodes with a branch support below 95% are marked with a grey dot. Mitochondrial genomes generated in this study are marked with an asterisk.

12

320   The median-joining haplotype networks differentiated samples within clade G3 in greater detail

321   and in a more precise geographic context (Figures 4 & S6). They revealed the same three

322   subclades within the G3 clade. The HVRI and the cyt *b* networks were concordant both with

323   each other and with the phylogenetic reconstructions in the attribution of samples to the

324   different subclades, but exhibited slight discrepancies in the relation of clades to each other

325   and the positioning of samples within the clades. Subclade G3-X contained hamadryas

326   baboons from Ethiopia, Somalia, and Eritrea. Subclade G3-Z contained samples from

327   Ethiopia, Somalia, Djibouti, from the southern tip of Eritrea and the Arabian Peninsula.

328   Subclade G3-Y contained samples from Eritrea, eastern Sudan, the Arabian Peninsula and

329   the mummified sample MHNL 51000172. Individuals closely related to this mummified baboon

330   in the cyt *b* network were those from Sudan (on the Red Sea coast and in Senaar), Eritrea

331   (between 14.3-16.0N 36.7-39.0E), and the Arabian Peninsula (Figure S6), and in the HVRI

332   network samples from location "Bbr" (Barka Bridge, 15.6N 38.0E) in Eritrea (Figure 4).

333

334
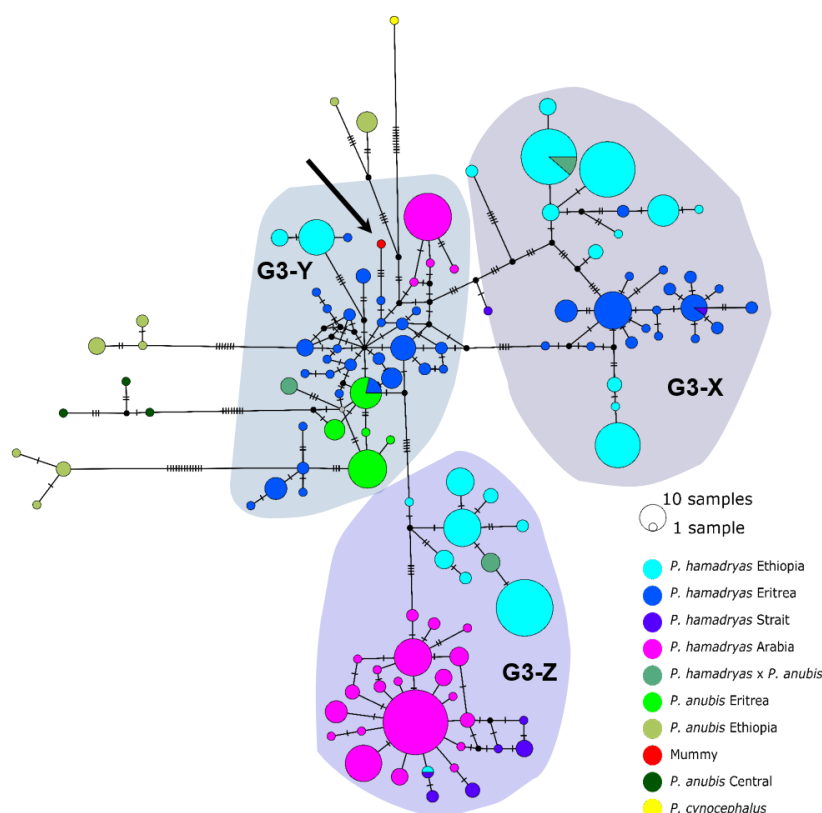
335   **Figure 4: Median joining haplotype network of north-eastern baboons** based on 644 D-loop sequences

336   (176bp). The analysed baboon mummy sample resolves in clade G3-Y (depicted in red, black arrow). Circle colour

337   reflects species and country of origin ("Arabia" comprises samples from Yemen and Saudi Arabia, "Strait"

338   comprises samples from near the Bab-el-Mandab Strait, i.e. southern Eritrea, Djibouti, northern Somalia).

13

Discussion

We succeeded in sequencing the mitogenomes of 14 modern historic baboons from north-eastern Africa and a mummified baboon recovered from Gabbanat el-Qurud, presenting the first genetic data of a mummified baboon from Ancient Egypt to date. DNA of the mummified baboon shows postmortem damage, which is, however, relatively low compared to what can be expected for samples of similar age (Dabney, Meyer, et al., 2013, Kistler et al., 2017). Low frequencies of post mortem damage were observed for aDNA from mummified specimens and have been attributed to the water deprivation during the mummification process, which may prevent hydrolytic deamination (Rossi et al., 2021). Postmortem damage observed here is within the range previously reported for aDNA derived from Egyptian human mummies (Schuenemann et al., 2017) and a Iranian saltmine sheep mummy (Rossi et al., 2021), which supports the authentic origin of our ancient sequence data and tends to rule out the possibility of contamination with modern DNA.

Our phylogenetic analysis of the newly generated mitogenomes in combination with published mitochondrial sequence data produced tree topologies in agreement with those of prior studies, with three well-supported clades across the north-eastern distribution of *Papio* (Roos et al., 2021). As previously described, introgressive hybridization has led to discordances between species assignment and mitochondrial clades (Rogers et al., 2019; Zinner et al., 2009, 2011). Our findings are notable for including specimens from previously unsampled and underrepresented regions, filling gaps in our knowledge of the distribution of mitochondrial clades. For instance, we report mitochondrial sequence data of baboons from regions previously uncovered, South Sudan and Sudan. We show that samples from South and southern Sudan, east of the White Nile, nest within the central olive baboon clade J, whereas samples from the coastal region of Sudan and east of the Blue Nile nest within the hamadryas clade G3. These findings expand the northern distributions of both clade J and clade G3 significantly, while also highlighting a strong geographic affinity between clade J and the Albertine Rift and (White) Nile Valley. Taxonomically, this clade corresponds with two subspecies recognized by Hill (Hill, 1970): *P. a. heuglini* and *P. a. tesselatum*.

A mummified hamadryas baboon from Gabbanat el-Qurud (MHNL 51000172) yielded sufficient aDNA to produce a complete mitogenome, which fell unequivocally in subclade G3-Y (cf. Kopp, Roos, et al., 2014). Haplotype networks allowed us to further refine subclade G3-Y, which consists of *P. hamadryas* and *P. anubis* samples from Eritrea and *P. anubis* samples from neighbouring regions in Sudan. G3-Y also includes samples from the southern-most distribution of *P. hamadryas* on the Arabian Peninsula. Geographic stability of phylogenetic clades over millennia has been shown for other baboon populations (Mathieson et al., 2020),

14

374   leading us to infer that MHNL 51000172 (or its maternal ancestor) originated in the region

375   where clade G3-Y exists today. We cannot completely rule out an Arabian origin for MHNL

376   51000172, as our data does not cover the entire historic and present haplotype diversity there,

377   but the tight clustering of the currently available Arabian sequences and distances in the HVRI

378   network make an Arabian origin of MHNL 51000172 unlikely. Similarly, the close relationship

379   with a sample of *P. anubis* from Sudan east of the Blue Nile (SMNS-Z-MAM-000584) could

380   indicate trafficking of baboons along the Nile, as suggested for specimens of *P. anubis*

381   recovered from Ptolemaic catacombs (Brandon-Jones & Goudsmit, 2022; Peters, 2020; von

382   den Driesch et al., 2004) and the Predynastic site of Hierakonpolis (Van Neer et al., 2004).

383   However, MHNL 51000172 was identified phenotypically as *P. hamadryas* (Lortet & Gaillard,

384   1907) and the distribution of hamadryas baboons is restricted to more eastern regions (Figure

385   2). If the distributions of baboons in north-eastern Africa have remained roughly stable within

386   the last 2500 years (as supported by ecological niche modelling (Chala et al., 2019)), the

387   region in Sudan east of the Blue Nile and west of the Atbarah River could not have served as

388   a source region for hamadryas baboons. Thus, it stands to reason that MHNL 51000172 (or

389   its maternal ancestor) was captured in present-day Eritrea (or close neighbouring regions) and

390   trafficked to Egypt. The value of this finding is twofold. First, it connects the mummified baboon

391   to populations that live today in Eritrea and eastern Sudan, between 13° and 20° latitude.

392   Second, our findings corroborate the reports of Greco-Roman historians, who described

393   Eritrea, and specifically Adulis as the sole source of *P. hamadryas* for Ptolemaic Egyptians.

394   Yet, this baboon predates the reign of Ptolemy I by centuries, presuming it is

395   contemporaneous with other baboons in the same assemblage, ca. 800–540 BCE. Thus, our

396   findings raise the possibility that Adulis already existed as a trading centre or entrepôt during

397   the 25th and 26th dynasties of Egypt. Although speculative, and expressed with due caution,

398   our reasoning would extend the antiquity of Egyptian–Adulite trade by as much as five

399   centuries.

400   Arguing for pre-Ptolemaic contact between Egypt and Adulis is fraught in the absence of

401   corroborating material evidence——but even so, the archaeological record is not entirely silent

402   on the prospect. Manzo (2010) and others (Zazzaro et al., 2014) have re-assessed the

403   ceramic tradition at Adulis and developed a chronology that stretches to the early second

404   millennium BCE, the deepest levels of which contained a fragment of blue glass with yellow

405   inlays similar to Egyptian glass from the New Kingdom (Fattovich, 2018). In Egypt, contact

406   with the Eritrean lowlands is attested by trade goods dating to ca. 1800–1650 BCE or earlier,

407   including potsherds, obsidian, and fragments of carbonized ebony (Fattovich, 2018; Lucarini

408   et al., 2020). Discovered at Mersa Gewasis, a Middle Kingdom harbour for launching seafaring

409   expeditions to the fabled Land of Punt (Bard & Fattovich, 2018), these Eritrean objects offer
410   tantalizing links between Punt and the prehistory of Adulis (Manzo, 2010, 2012).

411   Punt existed in a region south and east of Egypt, and was accessible by land or sea. For
412   Egyptians, Punt was a source of 'marvels', particularly incense, but also baboons, that drove
413   bidirectional trade for 1300 years (ca. 2500–1170 BCE) (Tallet, 2013). Some scholars have
414   described this enterprise as the beginning of economic globalization (Fattovich, 2012),
415   whereas others view it as the earliest maritime leg of the spice route (Keay, 2006), a trade
416   network that would shape geopolitical fortunes for millennia. The global historical importance
417   of Punt is therefore considerable, but there is a problem—its location is uncertain, in part
418   because the toponym fades from view. From the early first millennium BCE, there are no
419   further records of Egyptians in Punt, or of Puntites visiting Egypt. There are, however, two
420   incomplete inscriptions that mention Punt in a narrative context, and both are attributed to the
421   26th (Saite) Dynasty (Betrò, 1996; Cavasin, 2019). One of these, the Defenneh stele, describes
422   an expedition to Punt that was saved from dying thirst by unexpected rainfall on "the mountains
423   of Punt" (Meeks, 2003). The Defenneh stele is a testament to the efforts of Saitic pharaohs to
424   revive maritime commerce on the Red Sea (Lloyd, 1977), while also raising the possibility of
425   renewed trade with Punt. It is perhaps no coincidence that the Saite dynasty (664-525 BCE)
426   exists squarely within the radiometric date range of hamadryas baboons from Gabbanat el-
427   Qurud.

428   Punt, like Adulis, was a source of baboons for Egyptians, a history that raises the possibility
429   of using baboons as a tool for testing geographic hypotheses. Recently, Dominy et al. (2020)
430   used stable isotope mapping methods to determine the geoprovenance of mummified
431   baboons from Thebes (modern-day Luxor) and dated to the (late) New Kingdom. Their results
432   pointed to present-day Ethiopia, Eritrea, or Djibouti, as well as portions of Somalia, an area
433   that corroborates most scholarly views on the location of Punt (Breyer, 2016; Kitchen, 2004),
434   but see (Meeks, 2002, 2003; Tallet, 2013). Here, we used aDNA to show that at least one
435   baboon from the 25th Dynasty or Late Period of Egyptian history—a span that coincides with
436   the last known use of the toponym Punt, but predates Greco-Roman accounts of Adulis as a
437   source of baboons—can be traced to Eritrea. Thus, our findings appear to establish
438   primatological continuity between Punt and Adulis. Such a conclusion must be viewed with
439   caution, but it burnishes a longstanding current of conjecture among some historical
440   archaeologists: that Punt and Adulis were essentially the same trading centre from different
441   eras of Egyptian antiquity (Doresse, 1959; Fattovich, 2018; Kitchen, 2004; Massa, 2021;
442   Phillips, 1997; Sleeswyk, 1983).

443 At minimum, our results reinforce the view that ancient Egyptian mariners travelled great
444 distances to acquire living baboons. A great strength of this conclusion is that it is based on
445 distinct but complementary methods, but of course, the sample size is paltry and limited to *P.*
446 *hamadryas*, one of two baboon species recovered from Gabbanat el-Qurud. Moving forward,
447 it would be desirable to expand the sample size, examine specimens of *P. anubis* as well as
448 nuclear genomic data for increased precision, and include different time intervals of baboon
449 mummification.

450

451 **Future directions**

452 Direct radiocarbon dating of MHNL 51000172 and other baboons from Gabbanat el-Qurud is
453 an urgent priority, in part because doing so would put these specimens into conversation with
454 those from the catacombs of Tuna el-Gebel. The oldest gallery at Tuna el-Gebel, Gallery D,
455 is dated to the 26th Dynasty and contains a single species of baboon: *P. anubis*. Von den
456 Driesch and others (Peters, 2020; von den Driesch et al., 2004) have argued that these olive
457 baboons, as well as *Chlorocebus aethiops* (also found in Gallery D), were sourced from the
458 Sudanese Nile Valley and adjacent areas, which predicts membership in clade G3-Y, although
459 clade J is also plausible. Construction of Gallery C began during the first period of Persian rule
460 in Egypt (524-404 BCE) and continued through the 30th and Ptolemaic dynasties. As every
461 phase of Gallery C contains mummified specimens of both *P. anubis* and *P. hamadryas,* there
462 is rich opportunity to explore diachronic changes in trade routes using phylogeographic
463 methods. Uniform membership in clade G3-Y, for example, would affirm that Late Period
464 Egyptians were sourcing *P. hamadryas* from Eritrea as early as the sixth century BCE. Testing
465 this hypothesis may prove rewarding.

466

467 **Data access**

468 Raw sequencing data are deposited in the European Nucleotide Archive (ENA, project
469 accession no. PRJEB60261), mitochondrial genomes on Genbank (accession numbers:
470 OQ538075-OQ538089). Code used for data processing and analysis is available on OSF via
471 https://doi.org/10.17605/OSF.IO/D5GX3.

472

473

Acknowledgements

Author contributions

GHK conceived the study and collected the samples together with FG. FG coordinated and conducted lab work, supported by GHK and CR. FG and GHK analysed the data and wrote the first draft of the manuscript, GHK and NJD wrote the second draft of the manuscript. BH advised on and reviewed bioinformatic analyses. DB, CO, SP and WVN provided mummy samples and context information. JC and SM provided museum specimens. CR and DZ contributed to discussion about the interpretation of the data and the outline of the paper. GHK and CR provided laboratory space, equipment, and reagents. All authors contributed to the final manuscript.

18

References

507

508 Andrews, S. (2010). *FastQC: A quality control tool for high throughput sequence data*. Babraham Bioinformatics.

509   https://www.bioinformatics.babraham.ac.uk/projects/fastqc/

510 Bandelt, H.-J., Forster, P., & Röhl, A. (1999). Median-joining networks for inferring intraspecific phylogenies.

511   *Molecular Biology and Evolution*, *16*(1), 37–48.

512 Bard, K. A., & Fattovich, R. (2018). *Seafaring Expeditions to Punt in the Middle Kingdom: Excavations at*

513   *Mersa/Wadi Gawasis, Egypt*. BRILL.

514 Betrò, M. (1996). Punt, la XXVI dinastia e il frammento di statua del Museo Pushkin I.1.B 1025. *Egitto e Vicino*

515   *Oriente*, *19*, 41–49. http://www.jstor.org/stable/24233303

516 Bodenhofer, U., Bonatesta, E., Horejš-Kainrath, C., & Hochreiter, S. (2015). msa: an R package for multiple

517   sequence alignment. *Bioinformatics* , *31*(24), 3997–3999. https://doi.org/10.1093/bioinformatics/btv494

518 Boessneck, J. (1987). *Tuna el-Gebel I Die Tiergalerien*. Gerstenberg Verlag.

519 Bolger, A. M., Lohse, M., & Usadel, B. (2014). Trimmomatic: a flexible trimmer for Illumina sequence data.

520   *Bioinformatics*, *30*(15), 2114–2120. https://doi.org/10.1093/bioinformatics/btu170

521 Bowersock, G. W. (2013). *The Throne of Adulis: Red Sea Wars on the Eve of Islam*. OUP USA.

522 Brandon-Jones, D., & Goudsmit, J. (2022). The nonhuman primate remains from the baboon catacomb at

523   Saqqara in Egypt. In B. Urbani, D. Youlatos, & A. Antczak (Eds.), *World Archaeoprimatology.*

524   *Interconnections of Humans and Nonhuman Primates in the Past* (pp. 311–353). Cambridge University

525   Press, Cambridge, UK.

526 Breyer, F. (2016). *Punt: Die Suche nach dem "Gottesland."* BRILL.

527 Broad Institute. (2019). *Picard Toolkit*. http://broadinstitute.github.io/picard/

528 Burstein, S. M. (1989). *On the Erythraean Sea*. Hakluyt Society London.

529 Burstein, S. M. (2002). Kush, Axum and the ancient Indian Ocean trade. In T. A. Bács (Ed.), *A Tribute to*

530   *Excellence: Studies Offered in Honor of Ernö Gaál, Ulrich Luft, and Lásló Török* (pp. 127–137). Chaire

531   d'Egyptologie de l'Université Eotvos Lorand.

532 Casson, L. (1989). *The Periplus Maris Erythraei: Text with Introduction, Translation, and Commentary*. Princeton

533   University Press.

534 Casson, L. (1993). Ptolemy II and the Hunting of African Elephants. *Transactions and Proceedings of the*

535   *American Philological Association. American Philological Association*, *123*, 247–260.

536   https://doi.org/10.2307/284331

537 Cavasin, R. (2019). Tell Defenneh et la route de l'encens. *Égypte Nilotique et Méditerranéenne*, *12*, 1–24

538 Chala, D., Roos, C., Svenning, J.-C., & Zinner, D. (2019). Species-specific effects of climate change on the

539   distribution of suitable baboon habitats - Ecological niche modeling of current and Last Glacial Maximum

540   conditions. *Journal of Human Evolution*, *132*, 215–226. https://doi.org/10.1016/j.jhevol.2019.05.003

541   Dabney, J., Knapp, M., Glocke, I., Gansauge, M.-T., Weihmann, A., Nickel, B., Valdiosera, C., García, N., Pääbo,

542   S., Arsuaga, J.-L., & Meyer, M. (2013). Complete mitochondrial genome sequence of a Middle Pleistocene

543   cave bear reconstructed from ultrashort DNA fragments. *Proceedings of the National Academy of Sciences*

544   *of the United States of America*, *110*(39), 15758–15763. https://doi.org/10.1073/pnas.1314445110

545   Dabney, J., Meyer, M., & Pääbo, S. (2013). Ancient DNA damage. *Cold Spring Harbor Perspectives in Biology*,

546   5(7). https://doi.org/10.1101/cshperspect.a012567

547   Dominy, N. J., Ikram, S., Moritz, G. L., Wheatley, P. V., Christensen, J. N., Chipman, J. W., & Koch, P. L. (2020).

548   Mummified baboons reveal the far reach of early Egyptian mariners. *eLife*, *9*, e60860.

549   https://doi.org/10.7554/eLife.60860

550   Doresse, J. (1959). *Ethiopia*. Elek Books.

551   Edgar, R. C. (2004). MUSCLE: multiple sequence alignment with high accuracy and high throughput. *Nucleic*

552   *Acids Research*, *32*(5), 1792–1797. https://doi.org/10.1093/nar/gkh340

553   Fattovich. (2012). Egypt's trade with Punt: New discoveries on the Red Sea coast. *British Museum Studies in*

554   *Ancient Egypt and Sudan*.

555   Fattovich, R. (2018). The Archaeology of Punt. *The Journal of Egyptian Archaeology*, *104*(2), 205–209.

556   https://doi.org/10.1177/0307513319858321

557   Fauvelle-Aymar, F.-X. (2010). Les inscriptions d'Adoulis (Érythrée). Fragments d'un royaume d'influence

558   hellénistique et gréco-romaine sur la côte africaine de la mer Rouge. *Bulletin de l'Institut Français*

559   *D'archéologie Orientale - Tome 109*, *109*.

560   Geraads, D. (1987). Dating the Northern African cercopithecid fossil record. *Human Evolution*, *2*(1), 19–27.

561   https://doi.org/10.1007/BF02436528

562   Gippoliti, S. (2019). *Papio hamadryas* (e.T16019A17953082. Accessed on 23 August 2022.). The IUCN Red List

563   of Threatened Species . https://dx.doi.org/10.2305/IUCN.UK.2019-3.RLTS.T16019A17953082.en

564   Goudsmit, J., & Brandon-Jones, D. (1999). Mummies of Olive Baboons and Barbary Macaques in the Baboon

565   Catacomb of the Sacred Animal Necropolis at North Saqqara. *The Journal of Egyptian Archaeology*, *85*, 45–

566   53. https://doi.org/10.2307/3822426

567   Goudsmit, J., & Brandon-Jones, D. (2000). Evidence from the Baboon Catacomb in North Saqqara for a West

568   Mediterranean Monkey Trade Route to Ptolemaic Alexandria. *The Journal of Egyptian Archaeology*, *86*,

569   111–119. https://doi.org/10.2307/3822311

570   Hapke, A., Zinner, D., & Zischler, H. (2001). Mitochondrial DNA variation in Eritrean hamadryas baboons (*Papio*

571   *hamadryas hamadryas*): life history influences population genetic structure. *Behavioral Ecology and*

572   *Sociobiology*, *50*, 483–492.

573   Hatke, G. (2013). *Aksum and Nubia: Warfare, Commerce, and Political Fictions in Ancient Northeast Africa*. NYU

20

574   Press.

575   Hill, W. C. O. (1970). *Primates: Comparative Anatomy and Taxonomy* (Vol. 8). Edinburgh University Press.

576   Hoang, D. T., Chernomor, O., von Haeseler, A., Minh, B. Q., & Vinh, L. S. (2018). UFBoot2: Improving the

577   Ultrafast Bootstrap Approximation. *Molecular Biology and Evolution*, *35*(2), 518–522.

578   https://doi.org/10.1093/molbev/msx281

579   Huelsenbeck, J. P., & Ronquist, F. (2001). MRBAYES: Bayesian inference of phylogenetic trees. *Bioinformatics* ,

580   *17*(8), 754–755. https://www.ncbi.nlm.nih.gov/pubmed/11524383

581   Jolly, C. J., & Ucko, P. J. (1969). The riddle of the sphinx-monkey. *Man in Africa.* London: Tavistock.

582   Kalyaanamoorthy, S., Minh, B. Q., Wong, T. K. F., von Haeseler, A., & Jermiin, L. S. (2017). ModelFinder: fast

583   model selection for accurate phylogenetic estimates. *Nature Methods*, *14*(6), 587–589.

584   https://doi.org/10.1038/nmeth.4285

585   Keay, J. (2006). *The Spice Route: a history*. University of California Press.

586   Kitchen. (2004). The elusive land of Punt revisited. In P. Lunde & P. A. (Eds.), *Trade and travel in the Red Sea*

587   *region* (pp. 25–31). Argentum Press.

588   Kopp, G. H., Ferreira da Silva, M. J., Fischer, J., Brito, J. C., Regnaut, S., Roos, C., & Zinner, D. (2014). The

589   Influence of Social Systems on Patterns of Mitochondrial DNA Variation in Baboons. *International Journal of*

590   *Primatology*, *35*(1), 210–225. https://doi.org/10.1007/s10764-013-9725-5

591   Kopp, G. H., Roos, C., Butynski, T. M., Wildman, D. E., Alagaili, A. N., Groeneveld, L. F., & Zinner, D. (2014). Out

592   of Africa, but how and when? The case of hamadryas baboons (*Papio hamadryas*). *Journal of Human*

593   *Evolution*, *76*, 154–164. https://doi.org/10.1016/j.jhevol.2014.08.003

594   Korneliussen, T. S., Albrechtsen, A., & Nielsen, R. (2014). ANGSD: Analysis of Next Generation Sequencing

595   Data. *BMC Bioinformatics*, *15*, 356. https://doi.org/10.1186/s12859-014-0356-4

596   Leigh, J. W., & Bryant, D. (2015). popart : full-feature software for haplotype network construction. *Methods in*

597   *Ecology and Evolution / British Ecological Society*, *6*(9), 1110–1116. https://doi.org/10.1111/2041-

598   210X.12410

599   Li, H., & Durbin, R. (2009). Fast and accurate short read alignment with Burrows – Wheeler transform.

600   *Bioinformatics* , *25*(14), 1754–1760. https://doi.org/10.1093/bioinformatics/btp324

601   Li, H., Handsaker, B., Wysoker, A., Fennell, T., Ruan, J., Homer, N., Marth, G., Abecasis, G., Durbin, R., & 1000

602   Genome Project Data Processing Subgroup. (2009). The Sequence Alignment/Map format and SAMtools.

603   *Bioinformatics* , *25*(16), 2078–2079. https://doi.org/10.1093/bioinformatics/btp352

604   Lloyd, A. B. (1977). Necho and the Red Sea: Some Considerations. *The Journal of Egyptian Archaeology*, *63*(1),

605   142–155. https://doi.org/10.1177/030751337706300122

606   Lortet, L. C. E., & Gaillard, C. (1907). La faune momifiée de l'ancienne Egypte (deuxième série). *Archives du*

607   *Muséum d'histoire naturelle de Lyon*, *9*(1), 1–130. https://doi.org/10.3406/mhnly.1907.961

608   Lortet, L. C. E., & Gaillard, C. (1909). La faune momifiée de l'ancienne Egypte (troisième série). *Archives du*
609   *Muséum d'histoire naturelle de Lyon*, *10*, 1–9.

610   Lucarini, G., Barca, D., & Manzo, A. (2020). The provenance of obsidian artefacts from the Middle Kingdom
611   harbour of Mersa/Wadi Gawasis, Egypt, and its implications for Red Sea trade routes in the 2nd millennium
612   BC. *Quaternary International: The Journal of the International Union for Quaternary Research*, *555*, 85–95.
613   https://doi.org/10.1016/j.quaint.2020.03.015

614   Manzo, A. (2012). Nubians and the others on the Red Sea: An update on the exotic ceramic materials from the
615   Middle Kingdom harbour of Mersa/Wadi Gawasis, Red Sea, Egypt. In D. a. Agius, J. P. Cooper, A.
616   Trakadas, & C. Zazzaro (Eds.), *Navigated Spaces, Connected Places* (pp.47-58). Oxford: Archaeopress

617   Manzo, A. (2010). Adulis before Aksum? Possible 2nd and 1st millenium BC evidence from the site of the ancient
618   port. In G. Lusini (Ed.), *Current Trends in Eritrean Studies* (pp. 29–42). Università degli Studi di Napoli
619   "L'Orientale."

620   Massa, S. (2021). Eritrean Mobility and Cultural Heritage. New Frontiers of the Horn of Africa. In S. Bortolotto &
621   F. Cheli (Eds.), *Eritrean heritage: ancient routes and settlements* (pp. 47–61). Altralinea Edizioni.

622   Mathieson, I., Abascal, F., Vinner, L., Skoglund, P., Pomilla, C., Mitchell, P., Arthur, C., Gurdasani, D., Willerslev,
623   E., Sandhu, M. S., & Dewar, G. (2020). An ancient baboon genome demonstrates long-term population
624   continuity in southern Africa. *Genome Biology and Evolution*. https://doi.org/10.1093/gbe/evaa019

625   Meeks, D. (2002). Coptos et le chemin de Pount. *Topoi Supplément 3, Actes Du Colloque « Autour de Coptos »*
626   *Organisé Au Musée Des Beaux-Arts de Lyon (17-18 Mars 2000)*, 267–334.

627   Meeks, D. (2003). Locating Punt. In D. O'Connor (Ed.), *Mysterious Lands* (pp. 53–80). UCL Press.
628   https://doi.org/10.4324/9781843147626-4/locating-punt-dimitri-meeks

629   Munro-Hay, S. (1982). The foreign trade of the Aksumite port of Adulis. *Azania: Archaeological Research in*
630   *Africa*, *17*(1), 107–125. https://doi.org/10.1080/00672708209511302

631   Neukamm, J., Peltzer, A., & Nieselt, K. (2021). DamageProfiler: Fast damage pattern calculation for ancient
632   DNA. *Bioinformatics, 37*(20), 3652-3653. https://doi.org/10.1093/bioinformatics/btab190

633   Nguyen, L.-T., Schmidt, H. A., von Haeseler, A., & Minh, B. Q. (2015). IQ-TREE: a fast and effective stochastic
634   algorithm for estimating maximum-likelihood phylogenies. *Molecular Biology and Evolution*, *32*(1), 268–274.
635   https://doi.org/10.1093/molbev/msu300

636   Ottoni, C., Guellil, M., Ozga, A. T., Stone, A. C., Kersten, O., Bramanti, B., Porcier, S., & Van Neer, W. (2019).
637   Metagenomic analysis of dental calculus in ancient Egyptian baboons. *Scientific Reports*, *9*(1), 19637.
638   https://doi.org/10.1038/s41598-019-56074-x

639   Peters, J. (2020). The allochthonous fauna of Tuna el-Gebel and its cultural implications. In M. C. Flossmann-
640   Schütze, F. Hoffmann, & S. A. (Eds.), *Tuna el-Gebel — Eine Ferne Welt: Tagungsband zur Konferenz der*
641   *Graduate School "Distant Worlds" vom 16. bis 19.1.2014 in München* (pp. 253–267). Vaterstetten: Patrick

642   Brose.

643   Phillips, J. (1997). Punt and Aksum: Egypt and the Horn of Africa. *Journal of African History*, *38*, 423–457.

644   R Core Team. (2022). *R: A Language and Environment for Statistical Computing*. R Foundation for Statistical

645   Computing. https://www.R-project.org/

646   Richardin, P., Porcier, S., Ikram, S., Louarn, G., & Berthet, D. (2017). Cats, Crocodiles, Cattle, and More: Initial

647   Steps Toward Establishing a Chronology of Ancient Egyptian Animal Mummies. *Radiocarbon*, *59*(2), 595–

648   607. https://doi.org/10.1017/RDC.2016.102

649   Rogers, J., Raveendran, M., Harris, R. A., Mailund, T., Leppälä, K., Athanasiadis, G., Schierup, M. H., Cheng, J.,

650   Munch, K., Walker, J. A., Konkel, M. K., Jordan, V., Steely, C. J., Beckstrom, T. O., Bergey, C., Burrell, A.,

651   Schrempf, D., Noll, A., Kothe, M., … Baboon Genome Analysis Consortium. (2019). The comparative

652   genomics and complex population history of *Papio* baboons. *Science Advances*, *5*, eaau6947.

653   Rohland, N., Siedel, H., & Hofreiter, M. (2004). Nondestructive DNA extraction method for mitochondrial DNA

654   analyses of museum specimens. *BioTechniques*, *36*(5), 814–816, 818–821.

655   https://doi.org/10.2144/04365ST05

656   Ronquist, F., & Huelsenbeck, J. P. (2003). MrBayes 3: Bayesian phylogenetic inference under mixed models.

657   *Bioinformatics* , *19*(12), 1572–1574. https://doi.org/10.1093/bioinformatics/btg180

658   Roos, C., Knauf, S., Chuma, I. S., Maille, A., Callou, C., Sabin, R., Portela Miguez, R., & Zinner, D. (2021). New

659   mitogenomic lineages in *Papio* baboons and their phylogeographic implications. *American Journal of*

660   *Physical Anthropology*, *174*(3), 407–417. https://doi.org/10.1002/ajpa.24186

661   Rossi, C., Ruß-Popa, G., Mattiangeli, V., McDaid, F., Hare, A. J., Davoudi, H., Laleh, H., Lorzadeh, Z., Khazaeli,

662   R., Fathi, H., Teasdale, M. D., A'ali, A., Stöllner, T., Mashkour, M., & Daly, K. G. (2021). Exceptional ancient

663   DNA preservation and fibre remains of a Sasanian saltmine sheep mummy in Chehrābād, Iran. *Biology*

664   *Letters*, 17(7), 20210222. https://doi.org/10.1098/rsbl.2021.0222

665   Schubert, M., Ginolhac, A., Lindgreen, S., Thompson, J. F., Al-Rasheid, K. A. S., Willerslev, E., Krogh, A., &

666   Orlando, L. (2012). Improving ancient DNA read mapping against modern reference genomes. *BMC*

667   *Genomics*, *13*, 178. https://doi.org/10.1186/1471-2164-13-178

668   Schuenemann, V. J., Peltzer, A., Welte, B., van Pelt, W. P., Molak, M., Wang, C.-C., Furtwängler, A., Urban, C.,

669   Reiter, E., Nieselt, K., Teßmann, B., Francken, M., Harvati, K., Haak, W., Schiffels, S., & Krause, J. (2017).

670   Ancient Egyptian mummy genomes suggest an increase of Sub-Saharan African ancestry in post-Roman

671   periods. *Nature Communications*, *8*, 15694. https://doi.org/10.1038/ncomms15694

672   Seland, E. H. (2008). The Indian ocean and the globalisation of the ancient world. *Ancient West & East*, *7*(0), 67–

673   79. https://doi.org/10.2143/awe.7.0.2033253

674   Shapiro, B., & Hofreiter, M. (2013). *Ancient DNA* (pp. 475–481). Springer.

675   Sithaldeen, R. (2019). *Papio ursinus* (e.T16022A168568698 Accessed on 23 August 2022.). The IUCN Red List

676   of Threatened Species. https://dx.doi.org/10.2305/IUCN.UK.2019-3.RLTS.T16022A168568698.en

677   Sleeswyk, A. W. (1983). On the location of the land of Pwnt on two Renaissance maps. *International Journal of*

678   *Nautical Archaeology, 12.4,* 279-291.

679   Massicotte, P., & South, A . (2023). rnaturalearth: world map data from Natural Earth. R package version 0.1.0. .

680   https://docs.ropensci.org/rnaturalearth/https://github.com/ropensci/rnaturalearth.

681   Städele, V., van Doren, V., Pines, M., Swedell, L., & Vigilant, L. (2015). Fine-scale genetic assessment of sex-

682   specific dispersal patterns in a multilevel primate society. *Journal of Human Evolution*, *78*, 103–113.

683   Stadler, M. A. (2012). Thoth. *UCLA Encyclopedia of Egyptology*, *1*(1).

684   Tallet, P. (2013). Deux notes sur les expéditions au pays de Pount à la lumière de nouvelles données

685   archéologiques [PL. X-XI – PL. COUL. 13-15]. *Revue d'Égyptologie*, *64*(0), 189–209.

686   Tamura, K., & Nei, M. (1993). Estimation of the number of nucleotide substitutions in the control region of

687   mitochondrial DNA in humans and chimpanzees. *Molecular Biology and Evolution*, *10*(3), 512–526.

688   https://doi.org/10.1093/oxfordjournals.molbev.a040023

689   Tavaré, S. (1986). Some probabilistic and statistical problems in the analysis of DNA sequences. *Lectures on*

690   *Mathematics in the Life Sciences*, *17*(2), 57–86.

691   Trifinopoulos, J., Nguyen, L.-T., von Haeseler, A., & Minh, B. Q. (2016). W-IQ-TREE: a fast online phylogenetic

692   tool for maximum likelihood analysis. *Nucleic Acids Research*, *44*(W1), W232–W235.

693   https://doi.org/10.1093/nar/gkw256

694   Van Neer, W., Linseele, V., & Friedman, R. F. (2004). Animal burials and food offerings at the Elite Cemetery

695   HK6 of Hierakonpolis. In S. Hendrickx, R. F. Friedman, K. M. Cialowicz, & M. Chlodnicki (Eds.), *Egypt at its*

696   *Origins. Studies in Memory of Barbara Adams (Proceedings of the International Conference "Origin of the*

697   *State. Predynastic and Early Dynastic Egypt", Krakow, 28th August - 1st September 2002.)* (Vol. 1, pp. 67–

698   130).

699   von den Driesch, A., Kessler, D., & Peters, J. (2004). Mummified baboons and other primates from the Saitic-

700   Ptolemaic animal necropolis of Tuna El-Gebel, Middle Egypt. In G. Grupe & J. Peters (Eds.), *Documenta*

701   *Archaeobiologiae 2: Conservation policy and current research* (pp. 231–278). Rahden: Verlag Marie Leidorf.

702   Wallis, J. (2020a). *Papio anubis* (e.T40647A17953200 Accessed on 23 August 2022.). The IUCN Red List of

703   Threatened Species. https://dx.doi.org/10.2305/IUCN.UK.2020-2.RLTS.T40647A17953200.en

704   Wallis, J. (2020b). *Papio cynocephalus* (Version e.T92250442A92251260 Accessed on 23 August 2022). The

705   IUCN Red List of Threatened Species. https://dx.doi.org/10.2305/IUCN.UK.2020-

706   2.RLTS.T92250442A92251260.en

707   Wallis, J., Alonso, C., da Silva M. J., B. C. B. J. F., Hernansaiz A Kopp G, Vale, C., & Zinner, D. (2020). *Papio*

708   *papio. The IUCN Red List of Threatened Species* (No. e.T16018A17952926). IUCN.

709   https://doi.org/10.2305/IUCN.UK.2020-2.RLTS.T16018A17952926.en

710 Wallis, J., Petersdorf, M., Weyher, A.H. & Jolly, C.J. (2021). *Papio kindae* (e.T136848A190319676. Accessed on

711 23 August 2022.). The IUCN Red List of Threatened Species. https://dx.doi.org/10.2305/IUCN.UK.2021-

712 1.RLTS.T136848A190319676.en.

713 Wilkinson, J. G. (1853). *Topography of Thebes, and General View of Egypt: Being a Short Account of the*

714 *Principal Objects Worthy of Notice in the Valley of the Nile*. Murray. https://doi.org/10.11588/diglit.1035

715 Winney, B. J., Hammond, R. L., Macasero, W., Flores, B., Boug, A., Biquand, V., Biquand, S., & Bruford, M. W.

716 (2004). Crossing the Red Sea: phylogeography of the hamadryas baboon, *Papio hamadryas hamadryas*.

717 *Molecular Ecology*, *13*(9), 2819–2827. https://doi.org/10.1111/j.1365-294X.2004.02288.x

718 Yu, G., Smith, D. K., Zhu, H., Guan, Y., & Lam, T. T. Y. (2017). GGTREE: an R package for visualization and

719 annotation of phylogenetic trees with their covariates and other associated data. *Methods in Ecology and*

720 *Evolution*, *8*(1), 28–36. https://doi.org/10.1111/2041-210X.12628

721 Zazzaro, C., Cocca, E., & Manzo, A. (2014). Towards a Chronology of the Eritrean Red Sea Port of Adulis (1 ST -

722 Early 7 Th Century AD). *Journal of African Archaeology*, *12*(1), 43–73. http://www.jstor.org/stable/43135623

723 Zinner, D., Buba, U., & Roos, C. (2011). Pan-African voyagers: The phylogeography of baboons. In V. Sommer &

724 C. Roos (Eds.), *Primates of Gashaka. Socioecology and Conservation in Nigeria's Biodiversity Hotspot* (pp.

725 267–307). Springer.

726 Zinner, D., Groeneveld, L. F., Keller, C., & Roos, C. (2009). Mitochondrial phylogeography of baboons (*Papio*

727 spp.) - Indication for introgressive hybridization? *BMC Evolutionary Biology*, *9*, 83.

728 https://doi.org/10.1186/1471-2148-9-83

729 Zinner, D., Keller, C., Nyahongo, J. W., Butynski, T. M., de Jong, Y. A., Pozzi, L., Knauf, S., Liedigk, R., & Roos,

730 C. (2015). Distribution of Mitochondrial Clades and Morphotypes of Baboons *Papio* spp. (Primates:

731 Cercopithecidae) in Eastern Africa. *Journal of East African Natural History*, *104*(1-2), 143–168.

732 https://doi.org/10.2982/028.104.0111

733 Zinner, D., Wertheimer, J., Liedigk, R., Groeneveld, L. F., & Roos, C. (2013). Baboon phylogeny as inferred from

734 complete mitochondrial genomes. *American Journal of Physical Anthropology*, *150*, 133–140.

735 https://doi.org/10.1002/ajpa.22185

Table 1: Information on samples analysed in this study

Taxon	Origin	Museum ID	Country	Latitude	Longitude	MitoClade	AccNo	Reference
P. hamadryas	MNHN	MO-1972-357	ETH	9.320	42.119	G3-X	OQ538080	this study
P. hamadryas	SMNS	SMNS-Z-MAM-001034*	ETH	11.500	39.300	G3-X	OQ538076	this study
P. hamadryas	MfN	ZMB_Mam_025647_(2)	ETH	14.164	38.891	G3-X	OQ538079	this study
P. hamadryas	SMNS	SMNS-Z-MAM-000960	ERI	15.783	38.453	G3-X	OQ538078	this study
P. hamadryas	NHMUK	ZD.1910.10.3.1	SOM	9.933	45.200	G3-X	MT279063	Roos et al. 2020
P. hamadryas	MfN	ZMB_Mam_012808	ETH	9.314	42.118	G3-X	OQ538089	this study
P. anubis	Wild		ETH	8.968	38.571	G3-X	JX946196	Zinner et al. 2013
P. hamadryas	MfN	ZMB_Mam_042543_(1)	ETH	9.593	41.866	G3-Z	OQ538084	this study
P. hamadryas	MfN	ZMB_Mam_074849	DJI	11.589	43.129	G3-Z	OQ538085	this study
P. hamadryas	MNHN	MO-1972-359	ETH	6.998	40.478	G3-Z	OQ538086	this study
P. hamadryas	SMNS	SMNS-Z-MAM-001288	SDN	19.110	37.327	G3-Y	OQ538081	this study
P. hamadryas	Wild		ERI	15.011	38.971	G3-Y	JX946201	Zinner et al. 2013
P. hamadryas	SMNS	SMNS-Z-MAM-007509**	-	-	-	G3-Y	OQ538082	this study
P. hamadryas	MHNL	51000172	EGY	-	-	G3-Y	OQ538083	this study
P. anubis	SMNS	SMNS-Z-MAM-000584***	SDN	13.460	33.780	G3-Y	OQ538075	this study
P. cynocephalus	Wild		TNZ	-7.347	37.165	G1	JX946199	Zinner et al. 2013
P. cynocephalus	MNHN	ZM-MO-1977-5	SOM	3.243	45.471	G1	OQ538088	this study
P. anubis	NHMUK	ZD1929.4.27.2	COD	-0.800	26.633	J	MT279061	Roos et al. 2020
P. anubis	NHMUK	ZD1929.4.27.1	COD	-1.183	27.650	J	MT279062	Roos et al. 2020
P. anubis	Wild	19GNM2220916	TNZ	-4.679	29.621	J	MG787545	Roos et al. 2018
P. anubis	SMNS	SMNS-Z-MAM-032128	SSD	4.281	33.555	J	OQ538087	this study
P. anubis	SMNS	SMNS-Z-MAM-000583	SDN	13.333	32.729	J	OQ538077	this study
P. anubis	MfN	ZMB_Mam_074869	CMR	5.533	12.317	F	OQ538071	Kopp et al. in prep
P. anubis	Wild		NGA	7.317	11.583	F	JX946198	Zinner et al. 2013
P. anubis	MfN	ZMB_Mam_074887	CMR	9.328	12.946	F	OQ538069	Kopp et al. in prep
P. anubis	MfN	ZMB_Mam_074885	NGA	7.298	10.318	F	OQ538064	Kopp et al. in prep
P. anubis	MfN	ZMB_Mam_074883	CMR	6.334	9.961	F	OQ538072	Kopp et al. in prep
P. papio	Wild		SEN	12.883	-12.767	E	JX946203	Zinner et al. 2013
P. anubis	NHMUK	ZD.1947.586	SLE	8.917	-11.817	E	MT279064	Roos et al. 2020
P. anubis	MfN	ZMB_Mam_075043	TGO	9.260	0.781	D	OQ538066	Kopp et al. in prep
P. anubis	MfN	ZMB_Mam_011198	TGO	6.228	1.478	D	OQ538067	Kopp et al. in prep
P. anubis	Wild		CIV	8.800	-3.790	D	JX946197	Zinner et al. 2013
P. anubis	MfN	ZMB_Mam_007396_(1)	TGO	6.950	0.585	D	OQ538065	Kopp et al. in prep
P. anubis	NHMUK	ZD.1939.1022	NER	17.000	7.933	D	MT279065	Roos et al. 2020
P. anubis	NHMUK	ZD.1939.1020	NER	17.683	8.483	D	MT279066	Roos et al. 2020
P. anubis	MNHN	ZM-MO-1960-476	TCD	20.344	16.786	K	MT279067	Roos et al. 2020
P. anubis	MNHN	MO-1996-2511	CAF	3.905	17.922	K	OQ538068	Kopp et al. in prep
P. anubis	NHMUK	ZD.1907.7.8.11	CAF	8.000	20.000	K	MT279068	Roos et al. 2020
P. anubis	MNHN	MO-1996-2510	CAF	4.966	18.701	K	OQ538070	Kopp et al. in prep
P.ursinus	Wild		ZAF	-24.680	30.790	B	JX946205	Zinner et al. 2013
P. cynocephalus	Wild		TNZ	-11.261	37.514	B	JX946200	Zinner et al. 2013
P. kindae			ZMB	-12.591	30.252	C	JX946202	Zinner et al. 2013
P. cynocephalus	Wild	04MNM1300916	TNZ	6.119	29.730	H	MT279069	Roos et al. 2020
P. ursinus	Wild		ZAF	-34.456	20.407	A	JX946204	Zinner et al. 2013
P. cynocephalus	Wild	24UNF1150317	TNZ	7.815	36.895		MT279060	Roos et al. 2020
Theropithecus gelada							FJ785426	Hodgson et al. 2009

Abbreviations: AccNo, GenBank accession number; NHMUK, Natural History Museum, London; MNHN, Muséum National d'Histoire Naturelle, Paris; MfN, Museum für Naturkunde, Berlin; SMNS, State Museum of Natural History Stuttgart; MdC, Musée des Confluences, Lyon.
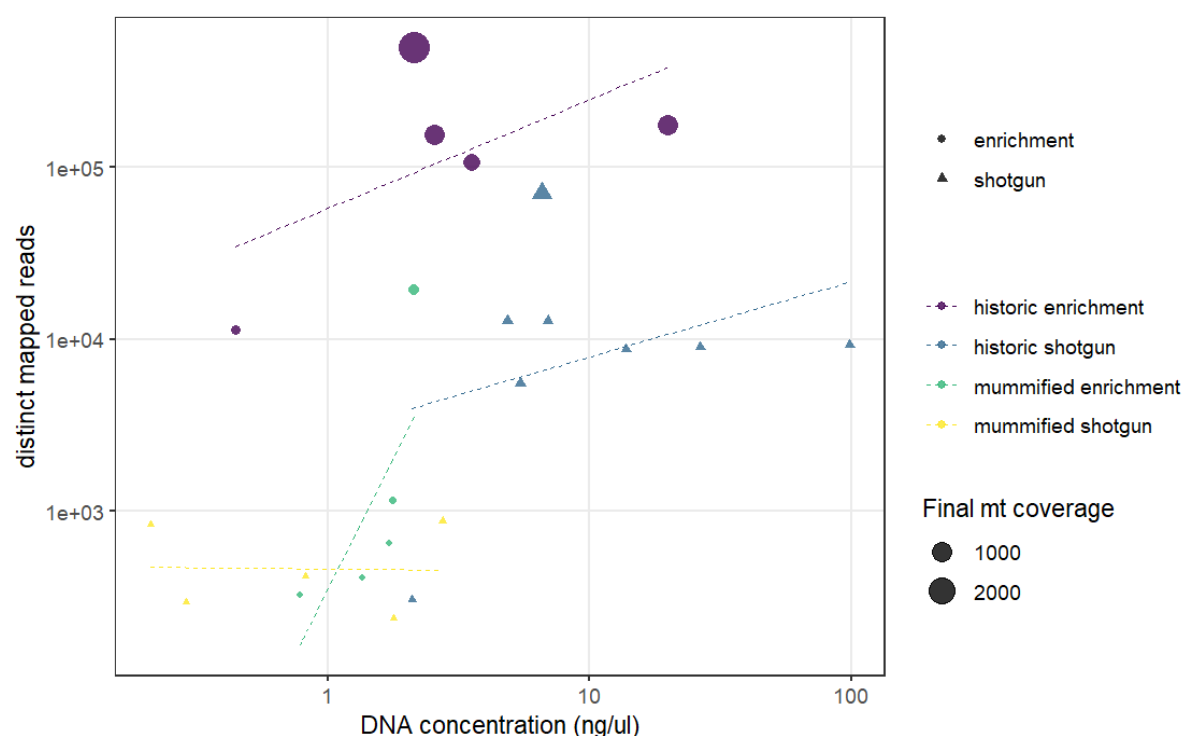
*mislabeled in museum records as *T. gelada*

**unclear provenance "Somaliland" (not equal to present-day Somaliland)

***misidentified provenance "Abyssinia" as Ethiopia in museum records

XXX: AccNo will be added upon acceptance of manuscript

Supplement

Figure S1: Comparison of DNA concentration and amount of distinct mapped reads. A higher DNA concentration produces a higher number of distinct mapped reads. Capture enrichment additionally increases the number of distinct mapped reads. Circles and triangles depict the different sequencing approaches, enrichment and shotgun, respectively; size is related to the final coverage of the mitogenome; colours represent the different sample types and sequencing approaches (yellow: shotgun sequencing of mummy sample, blue: shotgun sequencing of historic sample, purple: capture enrichment of historic sample, green: capture enrichment of mummy sample).
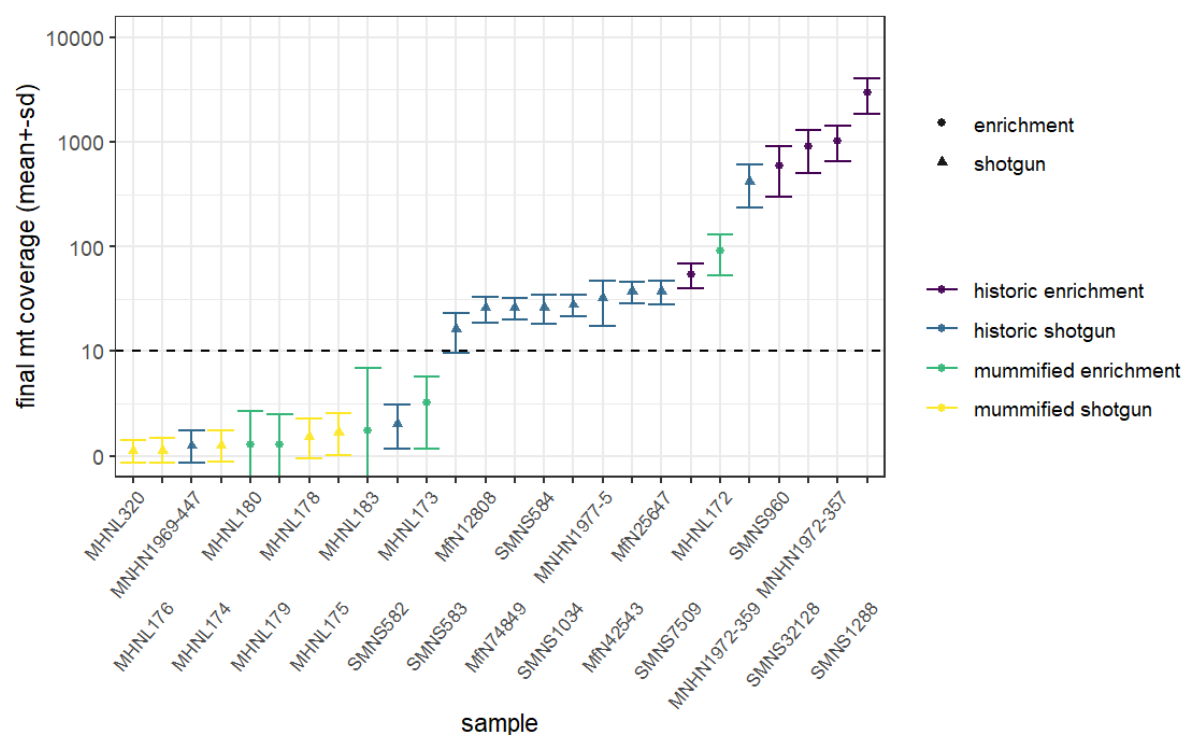
Figure S2: Overview of sequencing success for museum and mummy specimens. Mean (+- sd) final coverage of the mitogenome is shown for each sample (with abbreviated museum ID). Circles and triangles depict the different sequencing approaches, enrichment and shotgun, respectively; colours represent the different sample types and sequencing approaches (yellow: shotgun sequencing of mummy sample, blue: shotgun sequencing of historic sample, purple: capture enrichment of historic sample, green: capture enrichment of mummy sample). Dashed line shows the cut-off limit 10X for mean final coverage, samples below were excluded from final analyses.
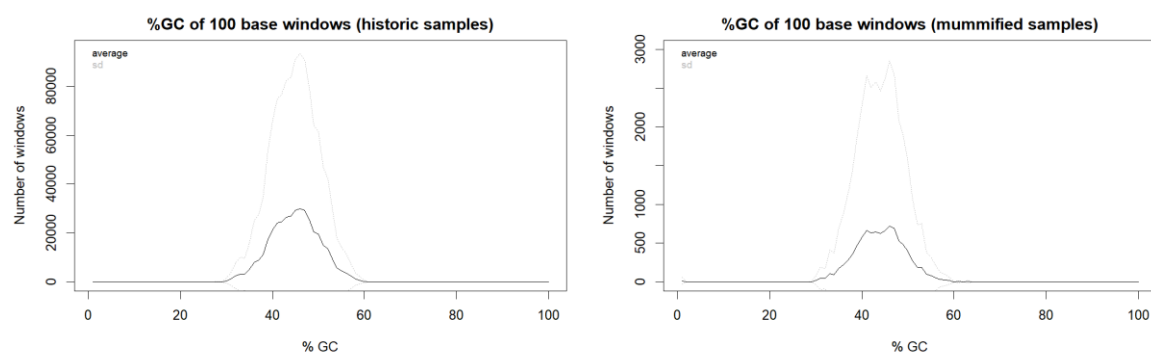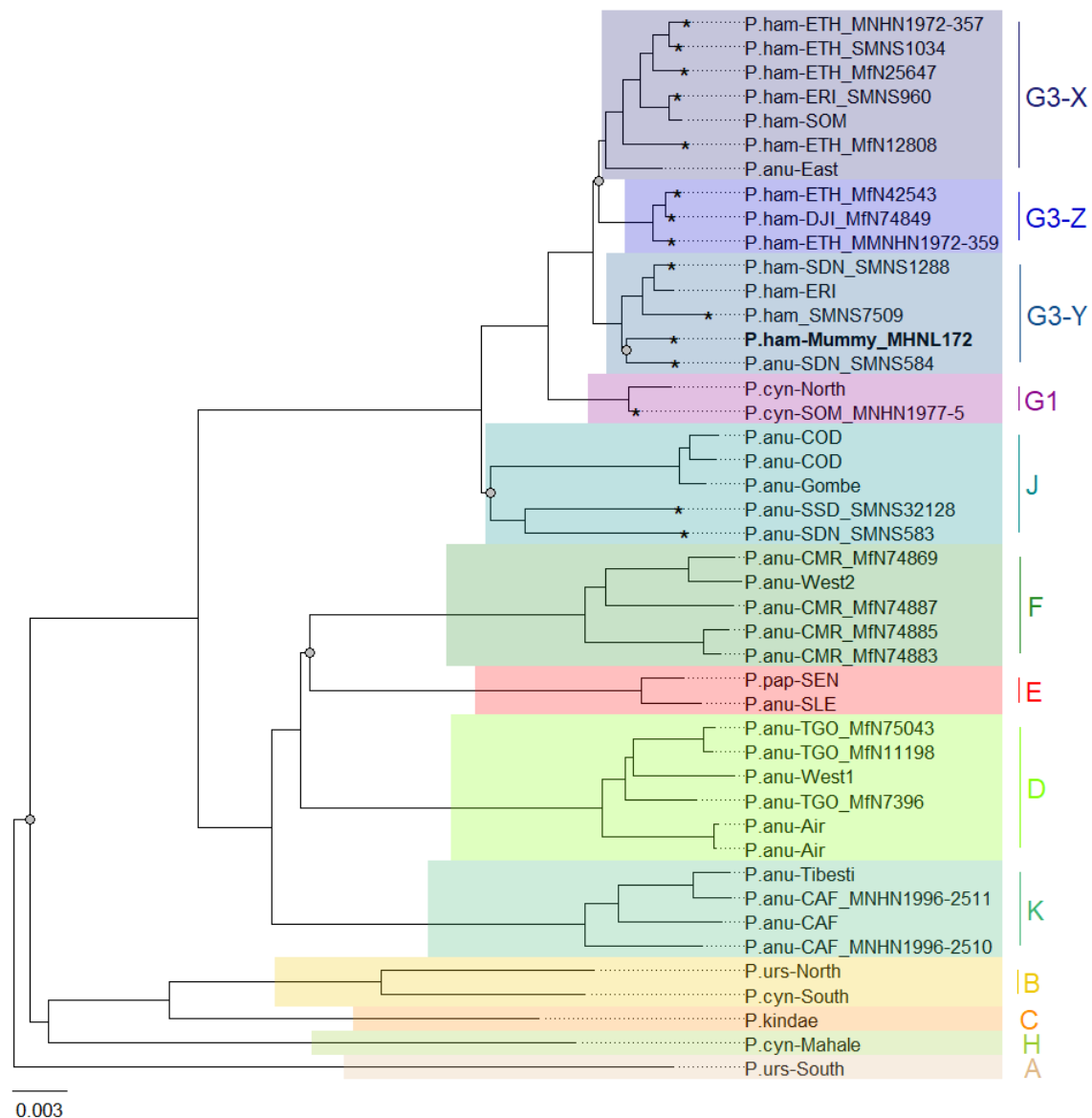
Figure S3: Distribution of GC content in historic samples and mummified samples.
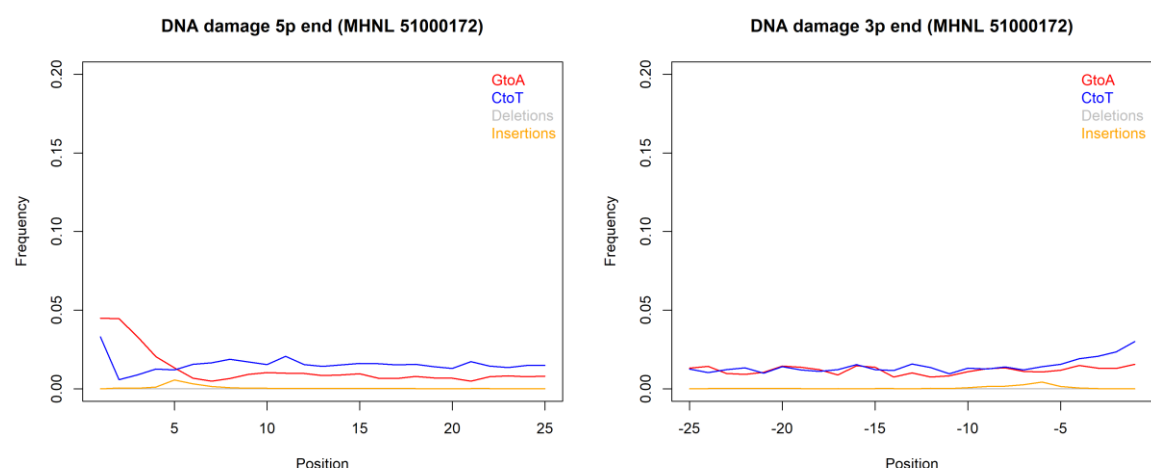
Figure S4: DNA damage plot for the sample of the mummified baboon MHNL 51000172 from 5' and 3' read ends, showing mean frequencies of C to T substitutions (blue), G to A substitutions (red), deletions (grey) and insertions (yellow) over the first/last 25 positions.

Figure S5: Phylogeny of baboons based on complete mitochondrial genomes under Bayesian inference. Outgroups (*T. gelada* and *P. cynocephalus*-Udzungwa) were omitted from visualization for clarity. The analysed baboon mummy sample MHNL 51000172 (in bold) falls into clade G3-Y. Clade names (A-K) according to Roos et al. (2020), subclades according to Kopp et al. (2014); sample IDs include putative species (P.ham - *P. hamadryas*, P.anu - *P. anubis*, P.cyn - *P. cynocephalus*, P.urs - *P. ursinus*, P.pap - *P. papio*), country of origin code (CAF - Central African Republic, CMR - Cameroon, COD - Democratic Republic of Congo, DJI - Djibouti, ERI - Eritrea, ETH - Ethiopia, NGA - Nigeria, SDN - Sudan, SSD - South Sudan, SEN - Senegal, SLE - Sierra Leone, SOM - Somalia, TGO - Togo; note that sample SMNS7509 is of unclear geoprovenance) and abbreviated museum code. Nodes with PP<95 are marked with a grey dot. Mitochondrial genomes generated in this study are marked with an asterisk.
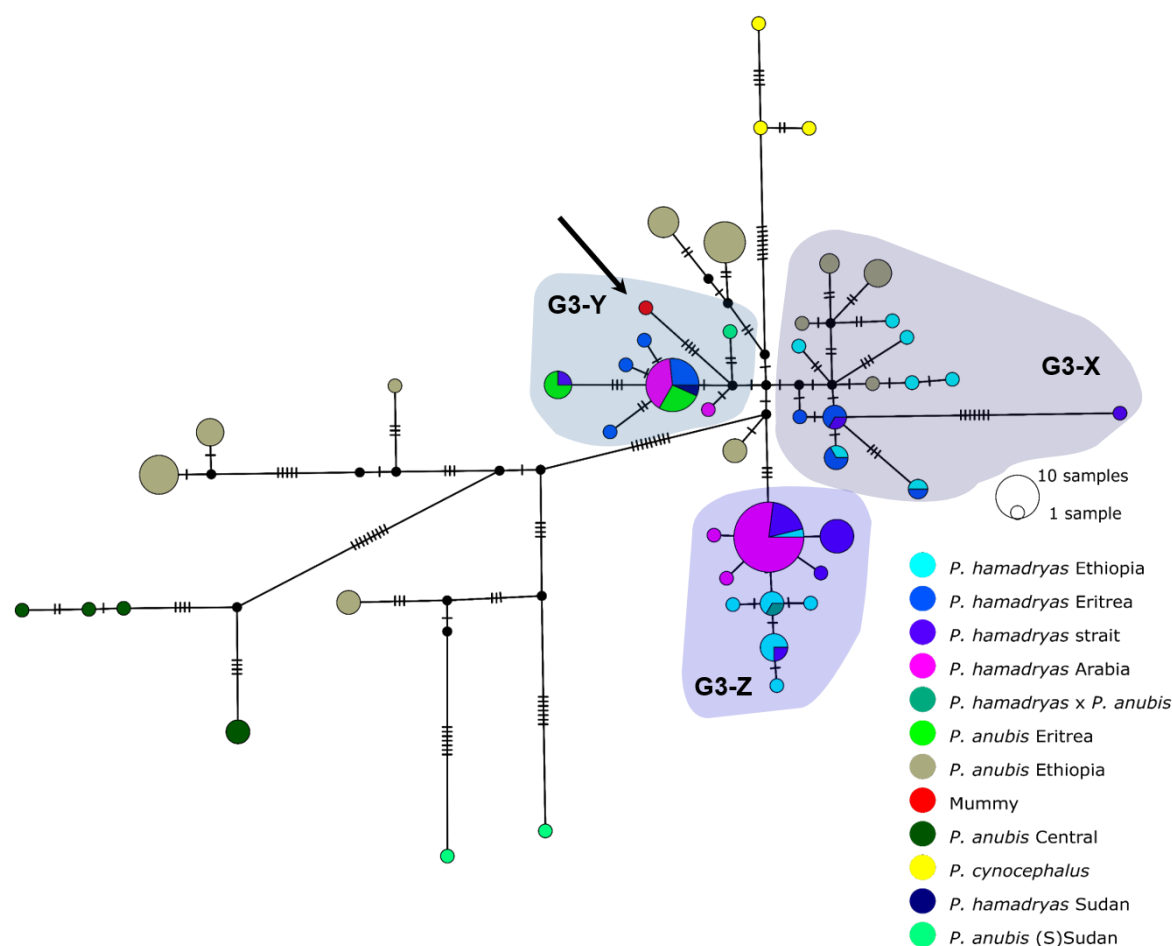
791

792   **Figure S6: Median joining haplotype network of north-eastern baboons** based on 137 cyt *b* sequences
793   (1140bp). The analysed baboon mummy sample resolves in clade G3-Y (depicted in red, arrow). Circle colour
794   reflects species and country of origin ("Arabia" comprises samples from Yemen and Saudi Arabia, "strait" comprises
795   samples from near the Bab-el-Mandab Strait, i.e. southern Eritrea, Djibouti, northern Somalia).

796

797   **Table S1:** Overview of analysed samples and sequencing results. (provided as .csv)